Improving Spectral Models By Unfolding Their Singularities

HAMPTON N. SHIRER[1] AND ROBERT WELLS[2]

The Pennsylvania State University, University Park 16802

(Manuscript received 7 August 1980, in final form 16 November 1981)

ABSTRACT

Maximally truncated spectral models have been used recently by fluid and atmospheric dynamicists to study nonlinear behavior of the governing partial differential system. However, too few external control parameters may be available in the truncated model to describe adequately the steady states near singular parameter values at which two or more stationary solutions meet. These missing parameters correspond in many cases to small but significant physical effects whose inclusion may be critically important for the model results to be realistic. We apply to truncated spectral models a recently developed contact catastrophe method that allows determination of the crucial physical effects that govern the steady states of a fluid system.

Spectral systems of three different fluid flow models of interest in atmospheric science are considered. Two parameters are necessary for modeling Rayleigh-Bénard convection. One represents the magnitude of the horizontal component, the other the magnitude of the vertical component of the externally imposed heating. Four parameters are required for modeling axisymmetric flow in either a rotating annulus or the atmosphere if the Prandtl number σ and the aspect ratio a are related by $\sigma a < 1$. These are the horizontal and vertical components of the external heating, the Coriolis parameter, and either the inclination angle of the vessel (annulus) or the Newtonian heating rate (atmosphere). Four parameters are essential for modeling quasi-geostrophic flow in a channel. They are the three Fourier coefficients of the Newtonian heating rate and the amplitude of a superimposed time-independent zonal current.

1. Introduction

A wide variety of nonlinear physical systems, including many encountered in fluid dynamics and atmospheric science, exhibit transitions from one type of flow to another. As the forcing is varied slowly, a new flow regime may replace the original one in a smooth manner. Such gradual transitions are found in Rayleigh-Bénard convection experiments as a two-dimensional roll replaces the conductive state (Krishnamurti, 1970a).

In some cases, however, a markedly different flow may suddenly replace the original one. These dramatic changes are often accompanied by hysteresis, which appears when the values of the controlling parameters at which the transition occurs depend on the history of the system. Fluid systems that are characterized by sudden changes in flow type and hysteresis include Rayleigh-Bénard convection (Krishnamurti, 1970b, 1973) and flow in a rotating annulus (Fultz *et al.*, 1959).

The atmosphere provides many examples of wave-like flows, ranging in scale from cloud streets to planetary waves. Moreover, these states are characterized by one or two wavenumbers in the horizontal and vertical (e.g., Sommeria and LeMone, 1978, for two-dimensional rolls). As seen in the laboratory prototypes, each of these flows can change form suddenly as the values of certain external parameters are varied.

Because the laboratory and atmospheric systems contain configurations dominated by only a few spatial harmonics, it is a reasonable hypothesis to suppose that truncated spectral models could represent correctly the most energetic part of these flows. The primary advantage of these models is that their nonlinear behavior can be investigated analytically and the fundamental physical causes of the transitions found.

In many cases, the observed transitions then correspond in the spectral model to new solutions branching from old ones as the values of certain external parameters are varied. Two or more solutions of a nonlinear differential system meet at a bifurcation, or singular, point at which linear stability is also exchanged between the two states. Thus, determination of the location of the singular points in the phase space of the model should provide insight into the physical causes of the observed transitions.

Some spectral models of convection have exhibited a sequence of sharp transitions that resembles qualitatively that observed in laboratory models (McLaughlin and Martin, 1975; Curry, 1978; Shirer and Dutton, 1979; Shirer, 1980). In addition, very low-

[1] Department of Meteorology
[2] Department of Mathematics

0022-4928/82/030610-12$07.00

order sets of equations representing either convective or large-scale atmospheric dynamics have been shown to contain an enormous variety of solutions and bifurcations. The structures of the solution surfaces in some of them provide simple explanations for hysteresis and sudden changes in the observed states (Lorenz, 1962, 1963; Veronis, 1966; Ogura and Yagihashi, 1970; McLaughlin and Martin, 1975; Curry, 1978, 1979; Vickroy and Dutton, 1979; Shirer and Dutton, 1979; Wiin-Nielsen, 1979; Boldrighini and Franceschini, 1979; Charney and Devore, 1979; Shirer, 1980; Mitchell and Dutton, 1981; Yost and Shirer, 1982).

If we accept the notion that low-order spectral models reproduce qualitatively the types of bifurcations typically found in fluid dynamical systems, then techniques should be sought by which truncated spectral models can be made most efficient. One long-term goal of our research is to find the smallest spectral model that can represent each observed transition in such systems as Rayleigh-Bénard convection or a rotating annulus.

The results of any mathematical model can be limited in at least two important ways. First, the number of equations in the set may be too small for the transitions of interest to appear. For example, spectral systems derived from two-dimensional partial differential equations cannot model the exchange of stability among steady two- and three-dimensional flows.

Second, the bifurcative behavior found in a particular set of nonlinear equations may not represent observations well because important external parameters were not included. Catastrophe theory developed by Thom (1976) addresses this issue, but for certain technical reasons it cannot be applied to the spectral models of atmospheric dynamics. For this reason, in a separate report (Shirer and Wells, 1982) summarized in the Appendix, we organize some powerful theorems of J. Mather (1968) into a nearly algorithmic procedure that can be applied to spectral models. We will refer to this version of Thom-Mather theory as contact catastrophe theory. To apply the theory, we examine the steady states in the neighborhood of a bifurcation, or singular, point and we determine whether or not the full range of possibilities are represented. When terms are added to the polynomial describing the steady states to bring it to its most general form, then the singularity is unfolded. With the use of this approach, we can ascertain when critical parameters are missing and, more significantly, where they must appear within the spectral system. This information often will lead to the identification of a missing physical parameter in the governing model equations. In this article, we show how the method can be used to make the description of steady states in some existing spectral models more realistic.

Physical evidence that this type of analysis is not merely a mathematical exercise is given for Rayleigh-Bénard convection by Tavantzis *et al.* (1978). They noted that some details of the branching convective solution found in Rayleigh-Bénard experiments cannot be reproduced adequately when only a vertical heating parameter is included. Heating that varies in the horizontal, although it may be weak, is always present in the laboratory models, and even small non-zero values of the horizontal thermal forcing can change markedly the qualitative behavior of the first bifurcation.

We discuss in the following three spectral models of fluid motion:

- Rayleigh-Bénard convection. Two thermal parameters must be included, one representing the imposed vertical and the other the imposed horizontal thermal gradients.
- Quasi-geostrophic flow in a channel. Four parameters are needed, three being the Fourier coefficients of the Newtonian heating rate and the last representing either the amplitude of the superimposed basic flow or the amplitude of the varying bottom topography.
- Axisymmetric states in the rotating annulus or atmosphere. Four parameters are required when the Prandtl number σ and the aspect ratio a are related by $\sigma a < 1$. They are the horizontal and vertical components of the externally imposed heating, the rotation rate of the vessel (or Coriolis parameter) and either the tilt angle of the domain (annulus) or the Newtonian heating rate (atmosphere).

In the next section we analyze the Lorenz model of Rayleigh-Bénard convection (Lorenz, 1963), and in the following section we discuss the other two spectral models. The contact catastrophe theory, together with definitions of all necessary terminology, is outlined in the Appendix. Extensions of the present approach to higher-order singularities are mentioned in the conclusions.

2. The Lorenz model of convection

The three-component spectral model of Lorenz (1963) is an important simple physical model primarily because it captures the essence of the first observed temporally-independent convective state. This system also has attracted much interest in recent years as a mathematical model of complicated aperiodic temporal flow (Marsden and McCracken, 1976). However, Marcus (1981) recently demonstrated via numerical integration of several different spectral systems that the temporal solutions found in the severely truncated models of Lorenz (1963), McLaughlin and Martin (1975), and Curry (1978) disappear and are replaced by stable steady states once the number of horizontal modes is increased sufficiently. Thus, the relevance of these temporal states to the physical system is in doubt.

Lorenz (1963) chose the original spectral truncation on the basis of numerical integrations of a much larger spectral system that were performed by Saltzman (1962), who found that the steady convective solutions were described adequately by only three spectral coefficients in some cases, even though more spectral degrees of freedom were available. Moreover, the magnitudes of the nontrivial steady states in the Lorenz model vary according to the relation $(R - R_s)^{1/2}$ in which R is the Rayleigh number and R_s is the value of the singular point at which branching occurs. This is the same functional form for the convective state that Chandrasekhar (1961, Appendix I) deduced from consideration of the energetics of the governing nonlinear Boussinesq equations alone.

The branching diagram for the Lorenz model is shown schematically in Fig. 1b, in which w^* represents the amplitude of the convective state, d_1 is $(R - R_s)/R_s$ and $d_1 = 0$ is the value of the singular point. According to the model results, either the upper or the lower branch can occur with equal probability; at a fixed location in the domain, one branch represents clockwise, the other counterclockwise, circulation.

Observed convection in the neighborhood of the critical Rayleigh number, however, is better represented by either the lower curve in Fig. 1a or the upper curve in Fig. 1c. The difference between the two solutions is again in circulation sense. The very sharp increase in amplitude depicted in Fig. 1b near $d_1 = 0$ is not seen, but rather a smoother transition is found. Travantzis *et al.* (1978) attribute this result to thermal noise in the bounding plates, which can be viewed as horizontal temperature variations along the boundaries. An alternate approach, discussed by Yost and Shirer (1982) is that horizontal temperature gradients introduced by the side boundaries are important. In this section we show how to use the contact catastrophe theory to conclude that a parameter in addition to the Rayleigh number is needed to describe fully the steady convective states, and we deduce that this new parameter can represent the magnitude of the horizontal heating.

a. The unfolding

In order to develop the perturbation convection equations, Lorenz first expressed the temperature field as

$$T = T_0 + \Delta T(z/H) + \Theta, \qquad (2.1)$$

in which ΔT is the magnitude of the imposed linear vertical temperature gradient and Θ is a perturbation that vanishes at the bottom and the top H of the domain. The basic temperature field then satisfies the conduction relation $\nabla^2 T = 0$. The nondimensional form of the two-dimensional, shallow Boussinesq equations used by Lorenz are

$$\frac{\partial}{\partial t^*}\tilde{\nabla}^2\psi^* = -K(\psi^*, \tilde{\nabla}^2\psi^*) + \sigma(1 + a^2)^{-1}\tilde{\nabla}^4\psi^* + \sigma(1 + a^2)\frac{\partial\Theta^*}{\partial x^*}, \qquad (2.2)$$

$$\frac{\partial\Theta^*}{\partial t^*} = -K(\psi^*, \Theta^*) + r\frac{\partial\psi^*}{\partial x^*} + (1 + a^2)^{-1}\tilde{\nabla}^2\Theta^*, \qquad (2.3)$$

in which the asterisk denotes a nondimensional variable, r is the normalized Rayleigh number $r = R/R_s$, a is the ratio of the domain height to width, σ is the Prandtl number (the ratio of viscosity and thermometric conductivity) and K denotes the Jacobian operator in the variables x^* and z^*.

The Lorenz system

$$\dot{x}_1 = -\sigma x_1 + \sigma x_2 = F_1, \qquad (2.4)$$

$$\dot{x}_2 = -x_1x_3 + rx_1 - x_2 = F_2, \qquad (2.5)$$

$$\dot{x}_3 = x_1x_2 - bx_3 = F_3, \qquad (2.6)$$

is obtained by substitution of

$$\psi^* = \sqrt{2}x_1 \sin x^* \sin z^*, \qquad (2.7)$$

$$\Theta^* = \sqrt{2}x_2 \cos x^* \sin z^* - x_3 \sin 2z^*, \qquad (2.8)$$

into (2.2)–(2.3), multiplication by the appropriate basis function and integration of the result over the domain $0 \leq x^* \leq n\pi$, $0 \leq z^* \leq \pi$. Here $b = 4(1 + a^2)^{-1}$. The value of the singular point at which branching occurs is given by $d_1 = r_s - 1 = 0$ (Fig. 1b).

Application of the contact catastrophe method outlined in the Appendix involves a judicious rewriting of (2.4)–(2.6) and then several simple algebraic calculations. Details are given in Shirer and Wells (1982). We find that the steady states of the Lorenz model (2.4)–(2.6) are the same as those of the transformed system

$$\mathbf{F}^*(\mathbf{v}^*, \mathbf{w}^*, \alpha_s) = \begin{pmatrix} v_1^* \\ v_2^* \\ q(w^*) \end{pmatrix}, \qquad (2.9)$$

in which $\alpha = (r, \sigma, b)$, $\sigma > 0$, $b > 0$ and $q(w^*) = -w^{*3}/b$.

From Table 2 in the Appendix we see that when the steady state polynomial consists of only a cubic term, then two parameters are needed to describe completely its solutions. For the Lorenz model, the singularity $\alpha_s = (1, \sigma, b)$ is unfolded, therefore, when we write

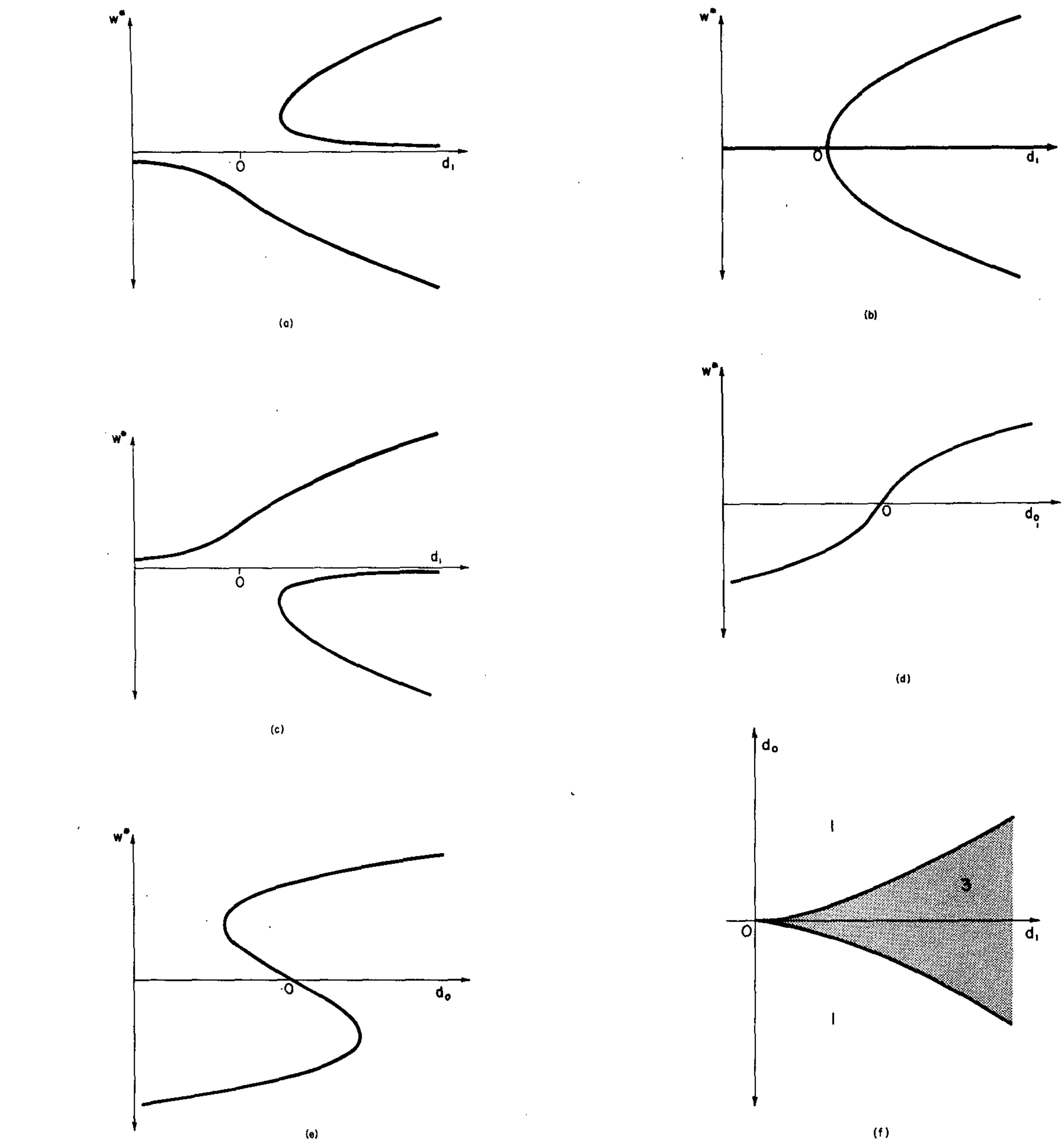

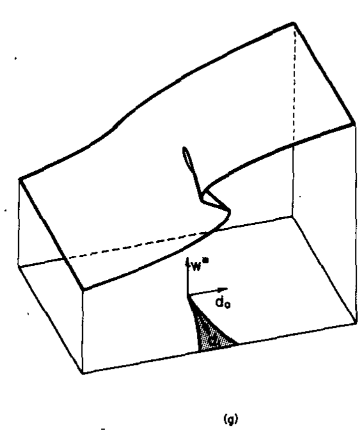

FIG. 1. Several ways in which the real-valued solutions of the cubic polynomial (2.10) can be displayed. First, the magnitude of the solution as a function of the linear coefficient d_1 is shown for the constant term $d_0 < 0$ (a), $d_0 = 0$ (b), and $d_0 > 0$ (c). Next, orthogonal cross sections are given for $d_1 < 0$ (d) and $d_1 > 0$ (e). The singularity set, a cusp, is displayed in (f); for values of d_0 and d_1 inside the set (shaded region), three real solutions to (2.10) exist, and for values outside the set, one real solution exists. Finally, in (g) the solution surface, which is the standard cusp surface, is shown as a function of both coefficients d_0 and d_1.

$$q(w^*) = -[(w^{*3}/b) - d_1 w^* - d_0]. \quad (2.10)$$

Solutions of (2.10) as functions of either d_0 or d_1 alone are shown schematically in Figs. 1a–e; the solutions in Figs. 1a–c, for which the value of d_1 varies, appear qualitatively different than those in Figs. 1d–e in which the value of d_0 varies. Evidently the parameter d_1 corresponds to the normalized Rayleigh number r because Fig. 1b contains the usual bifurcation picture. But from Figs. 1d–e we see that new qualitative behavior, hysteresis and sudden change, is possible for some values of d_1 ($d_1 > 0$) after d_0 has been introduced.

Transitions of either smooth or sudden type occur when two real roots of (2.10) meet. The parameter values that produce double roots comprise the singularity set, and for a cubic polynomial the set is given by

$$(d_0^2/4) - (d_1^3/27) = 0. \quad (2.11)$$

This is the equation for a cusp (Fig. 1f). For magnitudes of d_0 and d_1 inside the cusp (shaded region), three real solutions of (2.10) are possible, but for values outside the set, only one can exist. Three roots meet at the cusp point $d_0 = d_1 = 0$. Thus, all qualitatively important steady state behavior is summarized by the singularity set.

When the real solutions of (2.10) are drawn as functions of both the parameters d_0 and d_1, then we obtain the familiar cusp surface (Fig. 1g). From Figs. 1a–c and g we see that the Lorenz model solutions are given by the very special case $d_0 = 0$, and an arbitrarily small variation in the value of d_0 will cause the steady solutions to appear either as shown in Fig. 1a or c. Subsequent changes in the values of d_0, except $d_0 = 0$, will give again the same picture as in either Fig. 1a or c. Because specific values of any physical parameter cannot be set or maintained exactly, the bifurcative picture in Fig. 1b is unobservable. Thus, developing an interpretation for d_0 is crucial to our understanding of the physics of the problem.

b. *Physical interpretation*

Now that the two necessary parameters have been added in (2.10) to unfold about the singularity $r_s = 1$, we must find physical interpretations for them. We will show that d_1 represents vertical heating, or the Rayleigh number r, and that d_0 represents horizontal heating.

From (A11) we may write the unfolding (2.10) in the original system (2.4)–(2.6) as

$$F_1 = -\sigma x_1 + \sigma x_2 , \quad (2.12)$$

$$F_2 = -x_1x_3 + x_1 + (d_1 - 1)x_2 + d_0 , \quad (2.13)$$

$$F_3 = x_1x_2 - bx_3 , \quad (2.14)$$

By comparing (2.4)–(2.6) with (2.12)–(2.14) we see that a diabatic heating term d_0 has been added to (2.13), but that d_1 cannot represent the normalized Rayleigh number r in its present position. Thus, we prefer another version of $\mathbf{F}$.

First we write (2.12)–(2.14) in the form of (A12)

$$\begin{pmatrix} F_1 \\ F_2 \\ F_3 \end{pmatrix} = \begin{pmatrix} -\sigma x_1 + \sigma x_2 \\ -x_1x_3 + x_1 - x_2 \\ x_1x_2 - bx_3 \end{pmatrix} + d_1\begin{pmatrix} 0 \\ x_2 \\ 0 \end{pmatrix} + d_0\begin{pmatrix} 0 \\ 1 \\ 0 \end{pmatrix}. \quad (2.15)$$

We seek alternate column vectors as factors for d_1 and d_0. We find them by applying Mather's Contact Unfolding Theorem (A13) because (2.12)–(2.14) is a versal unfolding of (2.4)–(2.6). Thus

$$\begin{pmatrix} 0 \\ x_2 \\ 0 \end{pmatrix} = \begin{pmatrix} 0 & 0 & 0 \\ \sigma^{-1} & 0 & 0 \\ 0 & 0 & 0 \end{pmatrix} \times \begin{pmatrix} -\sigma x_1 + \sigma x_2 \\ -x_1x_3 + x_1 - x_2 \\ x_1x_2 - bx_3 \end{pmatrix} + \begin{pmatrix} 0 \\ x_1 \\ 0 \end{pmatrix} \quad (2.16)$$

and

$$\begin{pmatrix} 0 \\ 1 \\ 0 \end{pmatrix} = \begin{pmatrix} -\sigma & \sigma & 0 \\ 1 - x_3 & -1 & -x_1 \\ x_2 & x_1 & -b \end{pmatrix}\begin{pmatrix} 1/3 \\ -2/3 \\ -x_2(3b)^{-1} \end{pmatrix} + \begin{pmatrix} 0 & 0 & 0 \\ 0 & 0 & -(3b)^{-1} \\ -2(3\sigma)^{-1} & 0 & 0 \end{pmatrix} \times \begin{pmatrix} -\sigma x_1 + \sigma x_2 \\ -x_1x_3 + x_1 - x_2 \\ x_1x_2 - bx_3 \end{pmatrix} + \sigma\begin{pmatrix} 1 \\ 0 \\ 0 \end{pmatrix}. \quad (2.17)$$

From (2.16), (2.17) and the results of Mather's theory, we conclude that the steady states of (2.15) and the model with

$$F_1 = -\sigma x_1 + \sigma x_2 + d_0\sigma, \quad (2.18)$$

$$F_2 = -x_1x_3 + (d_1 + 1)x_1 - x_2 , \quad (2.19)$$

$$F_3 = x_1x_2 - bx_3 , \quad (2.20)$$

are governed by a cusp surface. Now the parameters d_0 and $d_1 = r - 1$ can be interpreted readily.

Because (2.18)–(2.20) does not admit of the trivial solution when $d_0 \neq 0$, we have that $x_1 \neq 0$ for each steady state. From (2.7) we conclude that $\psi^* \neq 0$, and therefore that steady fluid motion occurs even in the conductive case. From Jeffrey's theorem (Dutton, 1976), we know that whenever there are temperature gradients on a level surface, then motion must occur if there are no accelerations. From (2.2) we see that if the basic state temperature field varied in the horizontal, then an inhomogeneous term would appear in the vorticity equation. Because d_0 occurs in the spectral equation (2.18) originating from the vorticity equation, we may conclude that d_0 might represent basic horizontal heating.

This is indeed the case, as demonstrated by Yost and Shirer (1982), as long as the horizontal domain width corresponds to an odd multiple of π. The temperature field is now written as

$$T = T_0 + \Delta_z T(z/H) + \Delta_x T(ax/H) + \Theta \quad (2.21)$$

and the nondimensional horizontal heating parameter, the Hadley number h is defined here by

$$h = (\Delta_x T/\Delta_z T)r. \quad (2.22)$$

For the domain $0 \leqslant x^* \leqslant \pi$, $0 \leqslant z^* \leqslant \pi$, we obtain (Yost and Shirer, 1982)

$$\dot{x}_1 = -\sigma x_1 + \sigma x_2 - 8\sqrt{2}\sigma h/\pi^2, \quad (2.23)$$

$$\dot{x}_2 = -x_1 x_3 + r x_1 - x_2, \quad (2.24)$$

$$\dot{x}_3 = x_1 x_2 - b x_3 + \frac{8\sqrt{2}h}{3\pi^2} x_1, \quad (2.25)$$

By comparing (2.18)–(2.20) and (2.23)–(2.25), we can see that h and d_0 are proportional. However, to prove that (2.18)–(2.20) and (2.23)–(2.25) have the same steady state structure requires another application of Mather's Theorem (A13). Thus we now have the physical interpretation that the new parameter d_0 represents horizontal heating; we were led to it by using contact catastrophe theory.

We note from Fig. 1e that the parameter h, or d_0, introduces the possibility of hysteresis into the observed flow. This can only happen when $r > 1$ or $d_1 > 0$ (Figs. 1d–f). In Fig. 1e, the solution on the upper branch corresponds to circulation in one sense while that on the lower branch represents circulation in the opposite sense. When only one solution is possible, this circulation is always a direct one. Yost and Shirer (1982) show that these direct circulations are always stable. They also demonstrate that the solutions on the upper or lower branches change stability at the folds in some cases. From Fig. 1e we see that as the sign of the horizontal heating is changed, the circulation sense does not change sign simultaneously, and a thermally indirect flow is possible. Dramatic transitions from clockwise to counterclockwise flow will occur after a small change in the value of h (d_0) from inside to outside the singularity set (Fig. 1f) as the number of steady solutions decreases to one. These predictions could be tested in the laboratory.

Moreover, once d_0 has been added to the spectral system, the new model reproduces the observed behavior reported by Tavantzis *et al.* (1978). This improvement in model results was achieved by adding an external parameter rather than more spectral coefficients.

For values of the Rayleigh number near $r = 1$, we may conclude that all possible steady behavior is described by two control parameters. This result has its origins in the distribution of nonlinear terms in (2.4)–(2.6); the transformation of $\mathbf{F}$ to $\mathbf{F}^*$ in (2.9) produces a cubic term as the highest order one in $q(w^*)$. More parameters would be needed only if more nonlinear terms are present in the original spectral system so that $q(w^*)$ contained higher order terms. In the next section, we discuss two examples in which this occurs.

3. Butterfly points in the Rossby and Hadley regimes

Many low-order spectral models discussed in the literature have sufficient degrees of freedom that at least five different steady states are possible for the same fixed parameter values (e.g., Veronis, 1966; Vickroy and Dutton, 1979; Wiin-Nielsen, 1979; Boldrighini and Franceschini, 1979; Charney and Devore, 1979). In these systems there is the possibility that five equilibrium solutions may meet at a critical value of the external parameters called a butterfly point (Table 2). When a singularity of this type is present, four independent parameters would be needed to describe completely all transitions among the stationary solutions for parameter values in the neighborhood of the critical point.

In this section, we discuss the versal unfoldings of two truncated spectral models that contain butterfly points; each will require a fourth parameter, although the new control variables must be added in different ways in the two systems. Analysis of these models follows the procedure given in the Appendix. However, because the calculations are quite lengthy, we show here only the final results and interpret them physically. More details are given in Shirer and Wells (1982).

a. *Quasi-geostrophic flow*

The simplest nonlinear spectral model of quasi-geostrophic flow in a channel was studied by Vickroy and Dutton (1979). The Fourier coefficients are governed by

$$\dot{a}_1 = \Lambda_1 a_2 a_3 - \nu\lambda_1 a_1 - H_1/\lambda_1, \quad (3.1)$$

$$\dot{a}_2 = \Lambda_2 a_1 a_3 - \nu\lambda_2 a_2 - H_2/\lambda_2, \quad (3.2)$$

$$\dot{a}_3 = \Lambda_3 a_1 a_2 - \nu\lambda_3 a_3 - H_3/\lambda_3. \quad (3.3)$$

It can be shown using the Lyapunov-Schmidt procedure that the bifurcation point $H_1 = H_3 = 0$, $H_2 = \hat{H}_2$ is of cusp type, and so only two parameters are needed to unfold about the singularity. These two parameters can be associated via Mather's Contact Unfolding Theorem (A13) with either H_1 and H_2 or H_2 and H_3 in (3.1)–(3.3). Thus, inclusion of one of the heating coefficients in (3.1)–(3.3) is apparently unnecessary because it does not affect any of the transitions among the steady states near the bifurcation point $\hat{H}_2$.

However, when Vickroy and Dutton (1979) studied the singularity set of (3.1)–(3.3), they found that one, three, or five steady states were possible for different values of the thermal forcing. Because their system contains only cusp points, two solutions are always far from the other three and some important transitions between pairs of states cannot be modeled. Thus, the Vickroy and Dutton (1979) model is not as general as possible, and we need to find a suitable parameter that produces a butterfly point where all solutions meet.

Two physical effects that have been studied in the context of two-dimensional quasi-geostrophic flow are the barotropic instability of a basic zonal current $U(y)$ and topographic forcing. The latter effect was investigated recently with a truncated spectral model by Charney and Devore (1979). Introduction of either a nonlinear basic current $U(y)$ or a sinusoidally varying lower boundary into the quasi-geostrophic model will lead to a three-component system of the same form. With use of the Lyapunov-Schmidt procedure, it can be shown that three Newtonian heating parameters plus either the magnitude of the zonal current or the amplitude of the orography provide the necessary four parameters for the complete description of the transitions among the steady states. This model, therefore, is the appropriate one on which to begin studies of more complicated quasi-geostrophic systems.

The revised system has the form

$$\dot{a}_1 = \Lambda_1 a_2 a_3 - \nu\lambda_1 a_1 - H_1/\lambda_1 , \quad (3.4)$$

$$\dot{a}_2 = \Lambda_2 a_1 a_3 - \nu\lambda_2 a_2 + \Gamma_1 a_3 - H_2/\lambda_2 , \quad (3.5)$$

$$\dot{a}_3 = \Lambda_3 a_1 a_2 - \nu\lambda_3 a_3 - \Gamma_2 a_2 - H_3/\lambda_3 , \quad (3.6)$$

in which

$$\Gamma_1 = 3l\lambda_3|U|/8\lambda_2 , \quad (3.7)$$

$$\Gamma_2 = 3l\lambda_2|U|/8\lambda_3 , \quad (3.8)$$

are the Fourier coefficients of the zonal current $U(y) = -\partial\Psi(y)/\partial y = |U|(\pi^2/4 - y^2)$; the other variables are defined in Vickroy and Dutton (1979).

The singular point in the Vickroy and Dutton (1979) model (3.1)–(3.3) occurs on the H_2 axis. Indeed, for unforced inviscid models that conserve both energy and enstrophy, Mitchell and Dutton (1981) proved that forcing of only the largest or smallest scale cannot lead to instability, and so the bifurcations can occur only when intermediate forcing H_2 is present.

However, when the enstrophy constraint no longer applies, we find that more complicated branching may occur. The singular point in the revised model (3.4)–(3.6) occurs on the H_1 axis, and five steady states meet simultaneously at the singular point. In this example, then, forcing H_1 at the largest scale leads to more complicated instabilities than does forcing H_2 at the middle scale when a zonal current U of sufficient magnitude is introduced.

The existence of a butterfly singularity leads to the occurrence of many different types of transitions, and the existence of several different transition classes has important physical implications. Complicated hysteresis possibilities are introduced only when the fourth parameter, $|U|$, is added to the differential system. Because the steady states in (3.1)–(3.3) or (3.4)–(3.6) are governed by a quintic polynomial, further parameter additions will not lead to more complicated possibilities for the steady states. A less severe spectral truncation may admit of more general branching behavior; for example, the steady states of the five-component model of Wiin-Nielsen (1979) are governed by a ninth-degree polynomial.

To find the most general behavior of a system, we try to find enough critical values of the external parameters so that all but the highest order term in the steady state polynomial P vanish. In order to accomplish this, we sometimes have to add a parameter to the differential system before a lower order term of P can vanish. Executing this program with the Vickroy and Dutton (1979) model revealed important new stability results.

In the next example, however, the original system will contain enough degrees of freedom for the highest order singularity to be realized, but as in the Lorenz (1963) model example in Section 2, we will find that the interpretation of the entire unfolding will require that a new physical effect be identified.

b. *Axisymmetric flow*

Although the Coriolis parameter f is usually neglected in the shallow Boussinesq equations, there are physical systems in which f must be included. One is the axisymmetric or Hadley regime, in either the atmosphere or a rotating annulus. Because the periodic states of the Rossby regime are observed to develop from the steady axisymmetric states (Fultz *et al.*, 1959), a truncated spectral model designed to study these regime transitions must first be able to describe completely the branching behavior of the steady states themselves. This is studied most easily with a two-dimensional model; moreover, the appropriate maximally truncated spectral model is a natural extension of the modified Lorenz equations (2.23)–(2.25).

Once f has been introduced, we must add a v^* equation to the Boussinesq system. The simplest spectral system in which each variable, ψ^*, v^*, and Θ^*, occurs somewhere in a nonlinear term was studied by Veronis (1966), although he considered only the effects of vertical heating and rotation. His five-coefficient model can be specified by (2.7), (2.8) and

$$v^* = -\sqrt{2}x_4 \sin x^* \cos z^* + x_5 \sin 2x^*. \quad (3.9)$$

The steady states are governed by a quintic polynomial, and with the Lyapunov-Schmidt procedure it can be shown that the singularity is of butterfly type. Thus, four parameters must be used to unfold about the singularity; because Veronis (1966) only considered two of these, we must conclude that his model does not reproduce completely the transitions possible in the physical system.

With application of Mather's Contact Unfolding Theorem, we find that three of the four necessary parameters are the obvious ones: the Coriolis parameter f, the Rayleigh number r and the Hadley number h. However, there are 2 constant and 12 linear terms that serve as candidates for the location of the fourth parameter in the five-coefficient system. A parameter multiplying any of these terms is equivalent to any of the others because they lead to the same nonlinear behavior. However, the physical effects that create these terms will be markedly different in some cases, and this observation suggests a possible definition of dynamic similarity: Unfolded versions of physical systems are dynamically similar for parameter values near their singular points if their steady state structures are the same. For the present case of transitions among steady states (that is, those for corank 1 singularities), contact catastrophe theory shows that the steady state structure depends on the number of parameters in the unfolding. It therefore follows that physical systems are dynamically similar for parameter values in the neighborhood of their singularities if the number of parameters in the complete unfolding is the same, even though these parameters may be attributed to different physical effects in the two systems.

In the present five-component model, two of the possible locations are easy to interpret physically; the first is the tilt angle α of the domain, which leads to a buoyancy term with a horizontal component, and the second is diabatic heating of Newtonian type, which introduces an inhomogeneous term in one of the thermodynamic equations. The first corresponds to flow in a rotating annulus; because no laboratory vessel can be perfectly level, there is always a small angle α between the gravity vector and the vertical. However, Newtonian heating, which plays a critical role in the modeling of Rossby regime flows (Vickroy and Dutton, 1979), is the more suitable effect in an atmospheric β-plane model because the tilt angle is zero in this case.

These results suggest that the qualitative behavior of the atmospheric Hadley regime, which is affected by radiational heating as well as thermal boundary forcing, can be reproduced in the laboratory system simply by tilting the horizontally heated vessel. This is far easier to accomplish than to try to model the radiational heating itself. Thus we may use contact catastrophe theory to find ways to represent atmospheric effects indirectly in the laboratory by finding different physical parameters that lead to similar nonlinear qualitative behavior in the two systems. This search for equivalent effects that lead to dynamic similarity is often necessary when comparing laboratory and atmospheric flows; for example, the β-effect in the atmosphere is represented in a rotating annulus by radially varying fluid depth. This application of contact catastrophe theory to fluid systems might lead to improved and less expensive experimental design.

When a v^* equation, a lateral tilt angle α, and an inhomogeneous term q are added to the Boussinesq system (2.2)–(2.3), we have

$$\frac{\partial}{\partial t^*}\tilde{\nabla}^2\psi^* = -K(\psi^*, \tilde{\nabla}^2\psi^*) - f^*\frac{\partial v^*}{\partial z^*} + \sigma(1+a^2)^{-1} \times \tilde{\nabla}^4\psi^* + \sigma(1+a^2)\frac{\partial\Theta^*}{\partial x^*} - \sigma\alpha(1+a^2)a^{-1}\frac{\partial\Theta^*}{\partial z^*} + \sigma(1+a^2)h - \sigma\alpha(1+a^2)a^{-1}r, \quad (3.10)$$

$$\frac{\partial v^*}{\partial t^*} = -K(\psi^*, v^*) + f^*\frac{\partial\psi^*}{\partial z^*} + \sigma(1+a^2)^{-1}\tilde{\nabla}^2 v^*, \quad (3.11)$$

$$\frac{\partial\Theta^*}{\partial t^*} = -K(\psi^*, \Theta^*) + r\frac{\partial\psi^*}{\partial x^*} - h\frac{\partial\psi^*}{\partial z^*} + (1+a^2)^{-1}\tilde{\nabla}^2\Theta^* + q, \quad (3.12)$$

in which $f^* = fH^2\pi^{-2}\kappa^{-1}(1+a^2)^{-1}$ is a nondimensional form of f. Here we have assumed that the domain is not tilted in the y-direction and that α is small, so that the hydrostatic pressure field, constant density ρ_0 and α are related by $p_0(x, z) = p_{00} - \rho_0 gz - \rho_0 g\alpha x$. The unfolded version of the Veronis (1966) model obtained from substitution of (2.7), (2.8), and (3.9) into (3.10)–(3.12) is then (for the domain $0 \leqslant x^* \leqslant \pi$, $0 \leqslant z^* \leqslant \pi$)

$$\dot{x}_1 = -\sigma x_1 + \sigma x_2 + (16\sqrt{2}\sigma\alpha/3\pi^2 a)x_3 + f^*(1+a^2)^{-1}x_4 - 8\sqrt{2}\sigma(h - \alpha r a^{-1})\pi^{-2}, \quad (3.13)$$

$$\dot{x}_2 = -x_1x_3 + rx_1 - x_2 + 8\sqrt{2}q\pi^{-2}, \quad (3.14)$$

$$\dot{x}_3 = x_1x_2 - bx_3 + (8\sqrt{2}h/3\pi^2)x_1, \quad (3.15)$$

$$\dot{x}_4 = -x_1x_5 - f^*x_1 - \sigma x_4 , \quad (3.16)$$

$$\dot{x}_5 = x_1x_4 - \sigma ba^2x_5 . \quad (3.17)$$

For a complete unfolding, we retain either α or q, depending on which physical system we are studying.

The butterfly point is given by $\alpha = 0$ ($q = 0$), $h = 0$ and

$$r_c = -1/(\sigma^2a^2 - 1), \quad (3.18)$$

$$f_c^{*2} = -\sigma^4a^2(1 + a^2)/(\sigma^2a^2 - 1). \quad (3.19)$$

From (3.19) we see that this singular point exists only when $\sigma a < 1$ so that the four parameters are needed only when the inequality is satisfied. This leads to an important condition under which the laboratory and atmospheric flows are dynamically similar; because $\sigma a \ll 1$ in the atmosphere, only those laboratory systems for which $\sigma a < 1$ could serve as suitable models. Thus, a deep annulus containing water, such as the one used to develop the regime diagram in Fultz *et al.* (1959) (for which $a = 5.2$, $\sigma a = 36.4 \gg 1$), would not be adequate for modeling transitions within the atmospheric Hadley regime. In order to yield comparable branching results when water is the working fluid, a shallow annulus ($a < 0.1$) must be employed. Alternatively, a fluid such as mercury, for which $\sigma = 0.025$, might be used. These results demonstrate that a careful examination of the governing nonlinear equations must be performed in order to achieve dynamic similarity between the laboratory and atmospheric systems.

4. Conclusion

Clarification of the causes of transitions in nonlinear fluid flows is the paramount challenge facing fluid dynamics today. In the past, development of simple nonlinear models of such physical systems has proceeded in an *ad hoc* manner. Some physical insight into the causes of these transitions has been gained through study of truncated spectral models, but the relation between the truncated and full systems is still uncertain. Further progress can be gained only by anchoring the form of a spectral model in firm mathematical ground; applications of the developing theories of nonlinear mathematical structures provide approaches for pursuing this objective.

We have adopted the above philosophy as a means toward accomplishing our long-term goal: discovery of a sequence of generic truncated spectral models of physical systems that exhibit the transition to turbulence. The transition to turbulence is characterized typically by a sequence of bifurcations in flow type:

$$\text{motionless} \rightarrow \text{steady} \rightarrow \text{temporally periodic} \rightarrow \text{multiply periodic} \rightarrow \text{chaotic}.$$

[For a recent review of the subject, see Swinney and Gollub (1981)]. Each larger model in our proposed nested sequence would be able to reproduce one more of these transitions in addition to the previous ones.

In order to accomplish this task, we must consider both the choice of parameters and the truncation of basis functions. As a first step, we discuss here the consequences of parameter choice.

The observed states of a physical system will depend on different effects that appear in a complete mathematical model as the n parameters $\mu_1, \ldots, \mu_n$. However, only a subset $\{\mu_1, \ldots, \mu_m\}$ of these will control the transitions. The values of the m parameters $\mu_1, \ldots, \mu_m$ in the physical system are unlikely to be zero, and so a simplified version of the complete model can be expected to represent observable flow only when terms containing $\mu_1, \ldots, \mu_m$ are present in the model. When mathematical models are developed in an *ad hoc* manner, some of the crucial parameters may have been neglected inadvertently. This conclusion is illustrated by the study of Yost and Shirer (1982), who show that the form of the convective branch in a three-component spectral model of Rayleigh-Bénard convection agrees with observations (Tavantzis *et al.*, 1978) only after a horizontal heating parameter has been added. Thus, they found that simply adding a new parameter to the spectral differential system may improve the predictions of the resulting model more than could introducing additional equations into the system.

Therefore, objective methods for identifying the crucial parameters $\mu_1, \ldots, \mu_m$ are needed, and we present one possible mathematical procedure in the Appendix. Our procedure is based on finding the form of the branching solutions in the neighborhood of the value $\boldsymbol{\mu}_s$ of the parameters at which two or more solutions meet. The complete form of the multiple solutions, or the unfolding about the singularity $\boldsymbol{\mu}_s$, will contain a certain number of crucial parameters. These parameters represent the underlying causes of the transitions, and physical interpretation of these parameters is a key feature of our method.

The unfolding about $\boldsymbol{\mu}_s$ is determined by classifying $\boldsymbol{\mu}_s$ itself. This classification is accomplished in two stages: the first according to whether an eigenvalue or a complex conjugate pair of eigenvalues of the problem linearized about $\boldsymbol{\mu}_s$ changes sign as $\boldsymbol{\mu} - \boldsymbol{\mu}_s$ changes sign; the second, roughly speaking, according to how many eigenvalues, or complex conjugate pairs of eigenvalues, change sign simultaneously. In the first stage we find either branching time-independent states or branching periodic solutions (Hopf bifurcation), and in the second stage we obtain the specific unfolding.

We illustrate our ideas here by considering the first case of branching steady states for which only one eigenvalue vanishes at $\boldsymbol{\mu} = \boldsymbol{\mu}_s$, and we apply our procedure to spectral models of three different flows (Table 1). Use of this method is not limited to these three systems, however, because our general procedure applies to any finite dimensional system. More-

TABLE 1. Unfolded physical systems.

Physical system	Spectral model	Original critical parameters	Original physical effects	Singularity type	Number of parameters in unfolding	New parameters in unfolding	New physical effects
Rayleigh-Bénard convection	Lorenz (1963)	Rayleigh number R	Vertical heating	Cusp	2	Hadley number h	Horizontal heating
Quasi-geostrophic flow (Rossby regime)	Vickroy and Dutton (1979)	H_1 H_2	Components of Newtonian heating rate at smallest and middle wavenumbers.	Butterfly	4	H_3	Component of Newtonian heating rate at largest wavenumber.
						$\|U\|$ or h_0	Magnitude of zonal current or Amplitude of bottom topography
Rotating convection (Hadley regime)	Veronis (1966)	Rayleigh number R	Vertical heating	Butterfly	4	Hadley number h	Horizontal heating
		Coriolis parameter f	Rotation rate			Tilt angle α or q	Inclination of domain with respect to gravity or Newtonian heating rate

over, once the unfoldings have been determined for the higher-order singularities and Hopf bifurcations, the new required parameters can be interpreted physically in the same manner as that presented here.

Acknowledgments. We are grateful for the suggestions and encouragement provided by Professor John A. Dutton during the preparation of this article. We also wish to thank Professor John H. E. Clark, Dr. Kenneth Mitchell, and Mr. David Yost for their careful reading and suggested improvements of earlier versions of this manuscript. Finally, the many constructive criticisms of an anonymous reviewer helped us to improve the organization of the content of the article and to focus attention on the physical interpretation of our results.

The research reported here was partially funded by the National Science Foundation through grants ATM 78-02699 and ATM 79-08354 and the National Aeronautic and Space Administration through grants NSG-5347 and NAS8-33794.

APPENDIX

Outline of Contact Catastrophe Theory

We consider here systems of n nonlinear autonomous differential equations of the form

$$\frac{dx_i}{dt} = F_i(x_1, \ldots, x_n; \alpha_1, \ldots, \alpha_p),$$
$$i = 1, \ldots, n, \qquad \text{(A1)}$$

and we seek the properties of the set $S_1 = \{\mathbf{x}|\mathbf{F}(\mathbf{x}, \alpha) = 0\}$ of stationary points $\mathbf{x}_s$ of (A1) as the values of the external control parameters α_j are varied; for convenience, we assume that $\mathbf{x}_s = 0$ is a member of S_1 for all α_j. In particular, we seek the values of the singular points, or bifurcation points, $\boldsymbol{\alpha}_s$ at which two or more stationary solutions of (A1) meet. The collection of all singular points is called the singularity set.

The matrix $d\mathbf{F}(\mathbf{x}, \alpha) = (\partial F_i(\mathbf{x}, \alpha)/\partial x_j)$, when evaluated at $(0, \boldsymbol{\alpha}_s)$ has rank $r < n$ and corank $n - r$. The analysis is greatly simplified if we have a transformation that converts the first r equations of $\mathbf{F}$ to linear ones and that does not change either the number of stationary points in S_1 or the (topological) form of its singularity set. Then we may determine the properties of the singularity set by examining only the last $n - r$ nonlinear equations.

We accomplish this with use of parametric contact transformations of $\mathbf{F}$ of the form

$$\mathbf{U}(\mathbf{y}, \beta) = \mathbf{M}(\mathbf{y}, \beta)\cdot\mathbf{F}[\mathbf{x}(\mathbf{y}, \beta), \alpha(\beta)], \qquad \text{(A2)}$$

in which $\mathbf{M}$ is an $n \times n$ invertible matrix, for fixed β, $\mathbf{x}(\mathbf{y}, \beta)$ is a non-singular coordinate transformation $[\det(\partial x_i/\partial y_j) \neq 0$ at $\mathbf{y} = 0]$ and $\alpha(\beta)$ is a differentiable function of the new parameters β. We assume that the known value of $\boldsymbol{\alpha}_s$ corresponds to $\beta = 0$. Because $\mathbf{M}(0, 0) \neq 0$ and $\mathbf{x}(\mathbf{y}, \beta)$ are nonsingular, use of (A2) to transform $\mathbf{F}$ to $\mathbf{U}$ does not introduce more stationary points. Thus, both the number of stationary points in, and the composition of the singularity sets of, the sets S_1 and $S_2 = \{\mathbf{y}|\mathbf{U}(\mathbf{y}, \beta) = 0\}$ are the same. In this case, we say that $\mathbf{F}$ and $\mathbf{U}$ are (parametrically) contact equivalent.

To concentrate the nonlinear behavior of $\mathbf{F}$ into $n - r$ equations, we first express $\mathbf{x}$ as $(\mathbf{v}, \mathbf{w})$, in which $\mathbf{v}$ has r components and $\mathbf{w}$ has $n - r$ components. In doing this, we may have reordered $\mathbf{x}$. Then we rewrite $\mathbf{F}$ as

$$\mathbf{F}(\mathbf{v}, \mathbf{w}, \alpha_s) = \begin{pmatrix} \mathsf{A}(\mathbf{v}, \mathbf{w}) & \mathsf{B}(\mathbf{v}, \mathbf{w}) \\ \mathsf{C}(\mathbf{v}, \mathbf{w}) & \mathsf{D}(\mathbf{v}, \mathbf{w}) \end{pmatrix} \begin{pmatrix} \mathbf{v} \\ \mathbf{w} \end{pmatrix}, \quad \text{(A3)}$$

in which A is an $r \times r$ matrix of rank r, B is an $r \times (n - r)$ matrix, C is an $(n - r) \times r$ matrix, and D is an $(n - r) \times (n - r)$ matrix. Here, $\mathsf{A}(\mathbf{x})$ is invertible for all values of $\mathbf{x}$ near the origin $\mathbf{x} = 0$.

In catastrophe theory, the Gromoll-Meyer Splitting Lemma is used to reduce the system (A1) to one involving as few variables as possible. In the present case of contact catastrophe theory, the analogous reduction is carried out by the Lyapunov-Schmidt process, which provides a contact transformation from the function $\mathbf{F}$ of (A3) to a function $\mathbf{F}^*$ of the form

$$\mathbf{F}^*(\mathbf{v}^*, \mathbf{w}^*, \alpha_s) = \begin{pmatrix} \mathbf{v}^* \\ \mathbf{p}(\mathbf{w}^*) \end{pmatrix}. \quad \text{(A4)}$$

Here the function $\mathbf{p}(\mathbf{w}^*)$ is given by

$$\mathbf{p}(\mathbf{w}^*) = \mathsf{D}[\mathbf{v}^*(\mathbf{w}^*), \mathbf{w}^*] \cdot \mathbf{w}^* + \mathsf{C}[\mathbf{v}^*(\mathbf{w}^*), \mathbf{w}^*] \cdot \mathbf{v}^*(\mathbf{w}^*) \quad \text{(A5)}$$

and $\mathbf{v}^*(\mathbf{w}^*)$ is the solution of

$$\mathbf{v}^*(\mathbf{w}^*) + \mathsf{A}[\mathbf{v}^*(\mathbf{w}^*), \mathbf{w}^*]^{-1} \times \mathsf{B}[\mathbf{v}^*(\mathbf{w}^*), \mathbf{w}^*] \cdot \mathbf{w}^* = 0. \quad \text{(A6)}$$

It is evident that the existence of multiple stationary states of $\mathbf{F}^*$ is governed completely by the $n - r$ nonlinear equations $\mathbf{p}(\mathbf{w}^*) = 0$. Moreover, the denominators of $\mathbf{p}(\mathbf{w}^*)$ do not vanish in the neighborhoods of either the stationary point (0, 0) or the singular point α_s, so we need only consider the numerator $\mathbf{q}(\mathbf{w}^*) = [\mathbf{p}(\mathbf{w}^*)]$.

An intermediate step in the conversion of $\mathbf{F}$ to $\mathbf{F}^*$ is that $\mathbf{F}$ is contact equivalent to $\mathbf{F}_*$ of the form

$$\mathbf{F}_*(\mathbf{v}, \mathbf{w}, \alpha_s) = \begin{pmatrix} 1 & \mathsf{A}^{-1}\mathsf{B} \\ 0 & \mathcal{D} \end{pmatrix} \begin{pmatrix} \mathbf{v} \\ \mathbf{w} \end{pmatrix}, \quad \text{(A7)}$$

in which

$$\mathcal{D} = \mathsf{D} - \mathsf{C}\mathsf{A}^{-1}\mathsf{B}. \quad \text{(A8)}$$

Because the corank of $\mathbf{F}$ is $n - r$, the matrix $\mathcal{D}$ contains only zeros when $\mathbf{v} = \mathbf{w} = 0$. We note that when the co-rank is $n - r$, then $n - r$ eigenvalues vanish at the singularity, but, except for the case $n - r = 1$, when $n - r$ eigenvalues vanish simultaneously, the co-rank may be less than $n - r$. In practice, (A8) may be used to verify that the matrices A–D in (A3) have been chosen correctly before the final form (A4) of $\mathbf{F}^*$ has been calculated.

We now limit our discussion to the corank 1 case so that $\mathbf{q}(\mathbf{w}^*) = q(w^*)$. Typically, $q(w^*)$ will have the form

$$q(w^*) = a_l w^{*l} + a_{l-1} w^{*(l-1)} + \cdots + a_{l-m} w^{*(l-m)} = 0. \quad \text{(A9)}$$

TABLE 2. Corank 1 Unfoldings.

Highest order term	Type	Order d of singularity	Unfolding
Quadratic	Fold	1	$z^2 - d_0 = 0$
Cubic	Cusp	2	$z^3 - d_1 z - d_0 = 0$
Quartic	Swallowtail	3	$z^4 - d_2 z^2 - d_1 z - d_0 = 0$
Quintic	Butterfly	4	$z^5 - d_3 z^3 - d_2 z^2 - d_1 z - d_0 = 0$
Sixth Degree	Wigwam	5	$z^6 - d_4 z^4 - d_3 z^3 - d_2 z^2 - d_1 z - d_0 = 0$

Because at least two stationary solutions meet at $\alpha = \alpha_s$, we have that $l - m > 1$. The significant conclusion from Mather's Contact Unfolding Theorem (Mather, 1968) is that the graph of $q = 0$ will behave as the graph of the low-order term $w^{*(l-m)} = 0$ in the neighborhood of the singular point α_s. Accordingly, we can describe all possible steady states of $\mathbf{F}^*$, and therefore $\mathbf{F}$, by writing (A9) in its general form

$$q(w^*) = a_l w^{*l} + a_{l-1} w^{*(l-1)} + \cdots + a_{l-m} w^{*(l-m)} + \beta_d w^{*(d-1)} + \cdots + \beta_1 = 0, \quad \text{(A10)}$$

in which $d = l - m - 1$ is the degree of the singular point (Table 2). After adding the d parameters β_i, we say that the singular point α_s is versally unfolded. In the original system, this unfolding may be written as

$$\mathbf{F}(\mathbf{v}, w, \alpha_s, \beta) = \begin{pmatrix} \mathsf{A}(\mathbf{v}, w) & \mathsf{B}(\mathbf{v}, w) \\ \mathsf{C}(\mathbf{v}, w) & \mathsf{D}(\mathbf{v}, w) \end{pmatrix} \begin{pmatrix} \mathbf{v} \\ w \end{pmatrix} + \beta_1 \begin{pmatrix} 0 \\ 1 \end{pmatrix} + \beta_2 \begin{pmatrix} 0 \\ w \end{pmatrix} + \cdots + \beta_d \begin{pmatrix} 0 \\ w^{d-1} \end{pmatrix}. \quad \text{(A11)}$$

This is not yet a useful result in general because the spectral equations to which we apply this procedure contain no quadratic (w^2) or higher-order terms so that $\beta_3 - \beta_d$ in (A11) have no direct physical meaning. Also, the parameters β_1 or β_2 in (A11) may have no physical interpretation in their present position in the last equation of $\mathbf{F}$. Thus, we will seek other parametrically contact equivalent forms of (A11). The singularity sets of these alternate equations will be of the same form as those of (A11).

We can find the equivalent forms most efficiently through application of Mather's Contact Unfolding Theorem (Mather, 1968). According to this theorem, if

$$\mathbf{F}(\mathbf{x}, \alpha_s, \beta) = \mathbf{F}(\mathbf{x}, \alpha_s) + \mathbf{N}(\mathbf{x}) \cdot \beta \quad \text{(A12)}$$

is a versal unfolding of $\mathbf{F}(\mathbf{x}, \alpha_s)$, then any smooth n-component function $\mathbf{Y}(\mathbf{x})$ may be written (near $\mathbf{x} = 0$) as

$$\mathbf{Y}(\mathbf{x}) = d\mathbf{F}(\mathbf{x}, \alpha_s) \cdot \mathbf{G}(\mathbf{x}) + \mathbf{H}(\mathbf{x}) \cdot \mathbf{F}(\mathbf{x}, \alpha_s) + \mathbf{N}(\mathbf{x}) \cdot \gamma, \quad \text{(A13)}$$

in which the n-vector $\mathbf{G}(\mathbf{x})$, the $n \times n$ matrix $\mathbf{H}(\mathbf{x})$, and the n-vector γ depend on $\mathbf{Y}(\mathbf{x})$. It can be shown that (A11) is a versal unfolding of (A3); in this case the unfolding functions $\mathbf{N}_i(\mathbf{x})$ that together comprise the matrix $\mathbf{N}(\mathbf{x})$ are

$$\begin{pmatrix}0\\1\end{pmatrix},\ldots,\begin{pmatrix}0\\w^{d-1}\end{pmatrix}.$$

Because Mather's Theorem also works in reverse, we may use (A13) to find new unfolding functions $\mathbf{Y}_i$ to replace $\mathbf{N}_i$ in (A12). Provided that the vectors γ_i are each nontrivial, we may express each of the $\mathbf{N}_i(\mathbf{x})$ in the form (A13) as

$$\mathbf{N}_i(\mathbf{x}) = d\mathbf{F}(\mathbf{x}, \alpha_s)\cdot\mathbf{G}_i(\mathbf{x}) + \mathbf{H}_i(\mathbf{x})\cdot\mathbf{F}(\mathbf{x}, \alpha_s) + \mathbf{N}^*(\mathbf{x})\cdot\mu_i\,, \quad \text{(A14)}$$

in which now the column vectors $\mathbf{Y}_i$ together comprise the matrix $\mathbf{N}^*(\mathbf{x})$. In (A14), some columns of $\mathbf{N}$ and $\mathbf{N}^*$ may be the same. Then from Mather's theorem we may conclude that

$$\mathbf{F}(\mathbf{x}, \alpha_s, \Gamma) = \mathbf{F}(\mathbf{x}, \alpha_s) + \mathbf{N}^*(\mathbf{x})\cdot\Gamma \quad \text{(A15)}$$

is a new versal unfolding of $\mathbf{F}(\mathbf{x}, \alpha_s)$. The advantage of the new form (A15) over the original one (A12) is that the new functions $\mathbf{Y}_i$ will produce terms in the spectral equations that can be obtained through inclusion of certain other terms, which are multiplied by physically interpretable coefficients, in the governing partial differential system. By finding all possible new unfolding functions $\mathbf{Y}_i$ for each $\mathbf{N}_i$, we may determine all possible locations for new parameters; but only through use of physical reasoning can the realistic ones be identified. Thus, the mathematical procedure is a guide that focuses attention on the critical areas. Once all needed parameters are interpreted and inserted, the contact catastrophe theory ensures that all transitions among steady states can be described fully for all parameter values in the neighborhood of the singularity α_s.

REFERENCES

Boldrighini, C., and V. Franceschini, 1979: A five-dimensional truncation of the plane incompressible Navier-Stokes equations. *Commun. Math. Phys.*, **64**, 159–170.

Chandrasekhar, S., 1961: *Hydrodynamic and Hydromagnetic Stability*. Clarendon Press, 652 pp.

Charney, J. G., and J. G. Devore, 1979: Multiple flow equilibria in the atmosphere and blocking. *J. Atmos. Sci.*, **36**, 1205–1216.

Curry, J. H., 1978: A generalized Lorenz system. *Commun. Math. Phys.*, **60**, 193–204.

——, 1979: Chaotic response to periodic modulation of model of a convecting fluid. *Phys. Rev. Lett.*, **43**, 1013–1016.

Dutton, J. A., 1976: *The Ceaseless Wind: An Introduction to the Theory of Atmospheric Motion*. McGraw-Hill, 579 pp.

Fultz, D., R. R. Long, G. B. Owens, W. Boham, R. Kaylor and J. Weil, 1959: *Studies of Thermal Convection in a Rotating Cylinder with some Implications for Large-Scale Atmospheric Motions. Meteor. Monogr.*, No. 21, Amer. Meteor. Soc., 104 pp.

Krishnamurti, R., 1970a: On the transition to turbulent convection. Part I. The transition from two- to three-dimensional flow. *J. Fluid Mech.*, **42**, 295–307.

——, 1970b: On the transition to turbulent convection. Part 2. The transition to time-dependent flow. *J. Fluid Mech.*, **42**, 309–320.

——, 1973: Some further studies on the transition to turbulent convection. *J. Fluid Mech.*, **60**, 285–303.

Lorenz, E. N., 1962: Simplified dynamic equations applied to the rotating basin experiments. *J. Atmos. Sci.*, **19**, 39–51.

——, 1963: Deterministic nonperiodic flow. *J. Atmos. Sci.*, **20**, 130–141.

McLaughlin, J. B., and P. C. Martin, 1975: Transition to turbulence in a statically stressed fluid system. *Phys. Rev.*, **A12**, 186–203.

Marcus, P. S., 1981: Effects of truncation in modal representations of thermal convection. *J. Fluid Mech.*, **103**, 241–255.

Marsden, J. E., and M. McCracken, 1976: *The Hopf Bifurcation and Its Applications. Applied Mathematical Sciences*, Vol. 19. Springer-Verlag, 408 pp.

Mather, J., 1968: Stability of C^∞ mappings III: Finitely determined map germs. Institut Des Hautes Études Scientifiques, *Publ. Math.*, **35**, 127–156.

Mitchell, K. E., and J. A. Dutton, 1981: Bifurcations from stationary to periodic solutions in a low-order model of forced, dissipative, barotropic flow. *J. Atmos. Sci.*, **38**, 690–716.

Ogura, Y., and A. Yagihashi, 1970: A numerical study of finite-amplitude time-dependent convection induced by time-dependent internal heating: truncated systems. *J. Meteor. Soc. Japan*, **48**, 1–17.

Saltzman, B., 1962: Finite amplitude free convection as an initial value problem—I. *J. Atmos. Sci.*, **19**, 329–341.

Shirer, H. N., 1980: Bifurcation and stability in a model of moist convection in a shearing environment. *J. Atmos. Sci.*, **37**, 1586–1602.

——, and J. A. Dutton, 1979: The branching hierarchy of multiple solutions in a model of moist convection. *J. Atmos. Sci.*, **36**, 1705–1721.

——, and R. Wells, 1982: Mathematical structure of the singularities at the transitions between steady states in hydrodynamic systems. To be published either as a NASA Contractor Report under Grant Number NAS8-33794 and available from NTIS, Springfield, VA 22161 or as a volume in *Lecture Notes in Physics*, Springer-Verlag.

Sommeria, G., and M. LeMone, 1978: Direct testing of a three-dimensional model of the planetary boundary layer against experimental data. *J. Atmos. Sci.*, **35**, 25–39.

Swinney, H. L., and J. P. Gollub, 1981: *Hydrodynamic Instabilities and the Transition to Turbulence*. Springer-Verlag, 292 pp.

Tavantzis, J., E. L. Reiss and B. J. Matkowsky, 1978: On the smooth transition to convection. *SIAM J. Appl. Math.*, **34**, 322–337.

Thom, R., 1976: *Structural Stability and Morphogenesis*. W. A. Benjamin, 339 pp.

Veronis, G., 1966: Motions and subcritical values of the Rayleigh number in a rotating fluid. *J. Fluid Mech.*, **24**, 545–554.

Vickroy, J. G., and J. A. Dutton, 1979: Bifurcation and catastrophe in a simple, forced, dissipative, quasi-geostrophic flow. *J. Atmos. Sci.*, **36**, 42–52.

Wiin-Nielsen, A., 1979: Steady states and stability properties of a low-order barotropic system with forcing and dissipation. *Tellus*, **31**, 375–386.

Yost, D. A., and H. N. Shirer, 1982: Bifurcation and stability of low-order steady flows in horizontally and vertically forced convection. *J. Atmos. Sci.*, **39**, 114–125.